



Corrections in numerical methodology to evaluate plasticity induced crack closure along the thickness

J. Garcia-Manrique^{a,*}, D. Camas^a, M.E. Parrón-Rubio^b, A. Gonzalez-Herrera^a

^a Departamento de Ingeniería Civil, de Materiales y Fabricación, Universidad de Málaga, Escuela de Ingenierías. Spain

^b Departamento de Ingeniería Industrial y Civil, Universidad de Cádiz. Spain

ARTICLE INFO

Keywords:

Finite element analysis

Fatigue

PICC

Stress intensity factor

ABSTRACT

The influence of the three-dimensional effects of the distribution of the stress intensity factor in the numerical calculation of plasticity-induced crack closure is analysed in this paper. The usual methodology assumes a constant distribution of K along the thickness to obtain the effective stress intensity factor of the crack. This assumption should not be transposed to models that intend to observe phenomena in the crack front vicinity, where 3-D effects are a key aspect in the results. Through numerical simulations of both fracture and fatigue of through thickness straight cracks (CT specimen in mode I), the local opening and closure moment of each crack node is obtained and compared with previous one. Corrections are proposed for numerical methodology to obtain K_{op} and K_{cl} distribution along the thickness.

1. Introduction

One of the aims of fatigue design is to develop reliable methods of determining crack growth rate, in function of a given load parameter, that can be used to evaluate crack growth resistance for different applied stresses and different test piece and crack geometries. In 1963, Paris [1] introduced the stress intensity factor range to characterise the crack growth rate produced by cyclic variations in an applied stress field (where K_{max} and K_{min} are the maximum and minimum stresses applied during a fatigue cycle). Paris' law indicates stable crack growth at values above a given threshold (ΔK_{th}):

$$da/dN = C(\Delta K)^m = C(K_{max} - K_{min})^m \quad (1)$$

where, da/dN is the growth of the crack per fatigue cycle and C and m are material-specific constants that depend on factors such as microstructure, the load ratio ($R = K_{min}/K_{max}$) or environmental conditions.

Since then, authors have introduced modifications in order to consider other factors. For example, Walker [2] incorporated mean

stresses, while Forman's modification [3] not only accounted for mean stresses but also the curve's asymptotic effect for values of ΔK approaching K_{th} . Similarly, the literature contains a lot of approximations to these curves, such as those published by Smith [4] when fitting welding test results.

$$da/dN = C(\Delta K - \Delta K_{th})^m \quad (2)$$

Elber [5,6] introduced the theory that crack growth rate was dependent on the nature of the contact between the surfaces of the crack. Based on the assumption that crack propagation only occurs during the portion of the fatigue cycle when the crack is totally open, Elber suggested using the crack opening stress as a reference value to define the effective range of stresses and, subsequently, an effective range for the stress intensity factor (K_{eff}). Authors such as Ritchie and Suresh [7,8] later contributed with advances in the analysis of closure mechanisms. These developments included what is known as plasticity-induced crack closure (PICC).

Abbreviations: A, Crack length; b, Specimen's thickness; CT, Compact Tension specimen; E, Young's modulus; FE, Finite element analysis; K, Stress intensity factor; K_{cod} , Stress intensity factor due to COD method; K_J , Stress intensity factor due to J-integral method; K_{max} , Maximum stress intensity factor; K_{min} , Minimum stress intensity factor; K_N , Nominal stress intensity factor; K_{top} , Crack opening, tip tensile criterion; K_{rel} , Crack closure, tip tensile criterion; K_{ncop} , Crack opening, node contact criterion; K_{nec} , Crack closure, node contact criterion; P, Load applied; R, Stress ratio; r_{pd} , Dugdale's plastic zone size; W, Specimen's width; ΔK_{eff} , Effective range of stress intensity factor.

* Corresponding author.

Email addresses: josegmo@uma.es (J. Garcia-Manrique); dcp@uma.es (D. Camas); m.eugenia.parron@uca.es (M.E. Parrón-Rubio); agh@uma.es (A. Gonzalez-Herrera)

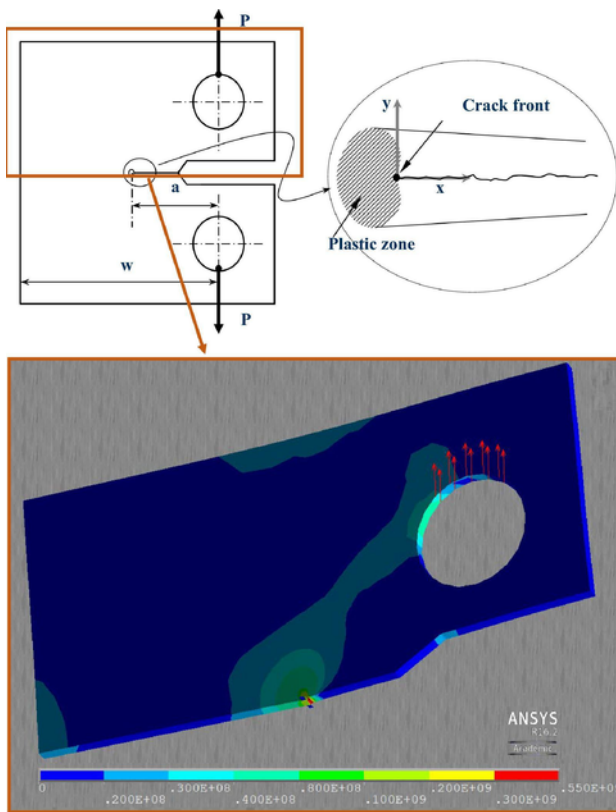


Fig. 1. schematic of the simulated CT compact tension specimen ($w = 50 \text{ mm}$, $a = 20 \text{ mm}$, $b = 3\text{--}9 \text{ mm}$) both in fracture and fatigue simulations.

$$\Delta K_{\text{eff}} = K_{\text{max}} - K_{\text{op}} = U \cdot \Delta K \tag{3}$$

$$da/dN = C \cdot \Delta K_{\text{eff}}^m \tag{4}$$

PICC models have used the plastic wake generated by the crack to describe the relationship between the loading-history effects and crack growth rate. A considerable amount of articles and studies have focused on this phenomenon and how it relates to other significant parameters, such as: the validity of PICC in the analysis of small crack growth [9]; analyses of overload effects on loading history [10–12]; numerical and experimental detection of crack opening and closure [13–15]; numerical modelling of the plastic wake [16,17]; its relationship with loading cycles in the presence of compressive loads [18,19]; etc.

Nonetheless, PICC still has its detractors [20,21]. Although the closure phenomenon has been observed experimentally and calculated numerically, the argument revolves around whether or not it actually has a genuine influence on crack propagation. Critics of PICC suggest growth is due to other driving forces acting in front of the crack, for example Kujawski [22] and Huang [23] have proposed solutions that depend on K_{max} and ΔK^+ (the positive part of ΔK). We consider pertinent to obtain good experimental correlations for the overall crack

growth rate by fitting the curves with different combinations of K , which still corresponds to the overall stress state at the crack tip. However, we believe that when the field of study is restricted to three-dimensional phenomena that take place in the vicinity of the crack front, then we should continue to assess the influence of PICC in each particular case.

Regarding this question, Antunes et al. [18,24] presented two very interesting articles in 2015. The first confirmed that the crack closure concept can explain growth even in the presence of compressive stresses. While the second study revealed the influence of PICC on the main crack front parameters. The latter paper also featured a comprehensive introduction and bibliography discussing the PICC phenomenon and aspects thereof which elicit contention among researchers. We are particularly interested in one of the disputed issues because it relates to the results presented herein; the uncertainty in the measurement (both experimental and numerical) of crack opening and closure values.

Indeed, there are unresolved problems regarding the experimental measurement of these values. There are notable differences between the results produced by classical treatments, as illustrated by the publications of Ashbaugh [25], Fleck et al. [26] and Ray et al. [27] who questioned the values or obtained 30% spreads in their analyses of U . In 1995, Yisheng and Schjive [28] concluded that the spread inherent to the methods used was around 10–15%. Authors such as Carrol et al. [29] or Mokhtarishirazabad et al. [30] have recently analysed the use of more accurate techniques such as Digital Image Correlation (DIC), although the results still present a certain degree of uncertainty. Furthermore, when examining parameters that vary across the thickness, the experimental methods are clearly limited by the fact that they only work on the visible side of the test specimen.

Therefore, numerical methods are particularly useful in this field of analysis. The correct numerical detection of crack closure during a fatigue process is a complex problem. Such a model must be able to analyse results at the crack front at singularity distances which feature significant gradients in the nodal solutions and important three-dimensional effects (Pook [31]). An added difficulty is the impossibility of validating the numerical results across the thickness with experimental tests. Hence the numerical model must be extremely and independently robust.

There is no consensus regarding the parameter that determines crack opening or closure instant during each fatigue cycle. The literature presents two clearly defined trends for determining crack opening. The first considers that the crack opens when there is no physical contact between the free surfaces (K_{nc}), which translates into the numerical model when the final or penultimate node in contact separates [32–34]. The second tendency, proposed by Sehitoglu and Sun [14,35], studies the stresses perpendicular to the plane of the crack at the crack tip (K_{tt}). Their first work defined the opening as the point at which the entire plane of the crack was placed under tension (K_t , tensile) [14]. Their subsequent paper [35] specified the moment at which the crack tip was placed under tension (K_{tt} , tip tensile). This represented a significant breakthrough in terms of analysing the results as it reduced the impact of mesh size on the crack tip environment.

The numerical determination of opening and closure was the main subject of Gonzalez-Herrera’s thesis [36] (2004). The main objective was to validate a numerical calculation method by identifying the in-

Table 1
Resume of mesh design parameters.

3-D models. $K_{\text{Nmax}} = 20 \text{ MPa m}^{1/2}$. Straight crack front.						
Simulation (year)	fatigue(2007)	fatigue(2007)	fatigue(2012)	fatigue(2012)	fracture(2015)	fracture(2017)
Thickness	3 mm	6 mm	3 mm	6 mm	3 mm	6 mm
Number of elements	37.838	64.016	82.546	102.710	60.374	120.223
Minimum element size (x axis): t_{mex}	42.86 μm	60 μm	10.32 μm	10.32 μm	11.85 μm	11.85 μm
Minimum element size (z axis): t_{mez}	10 μm	10 μm	17.5 μm	34.6 μm	40 μm	40 μm
Element shape ratio	4.3	6	1.7	3.35	3.37	3.37

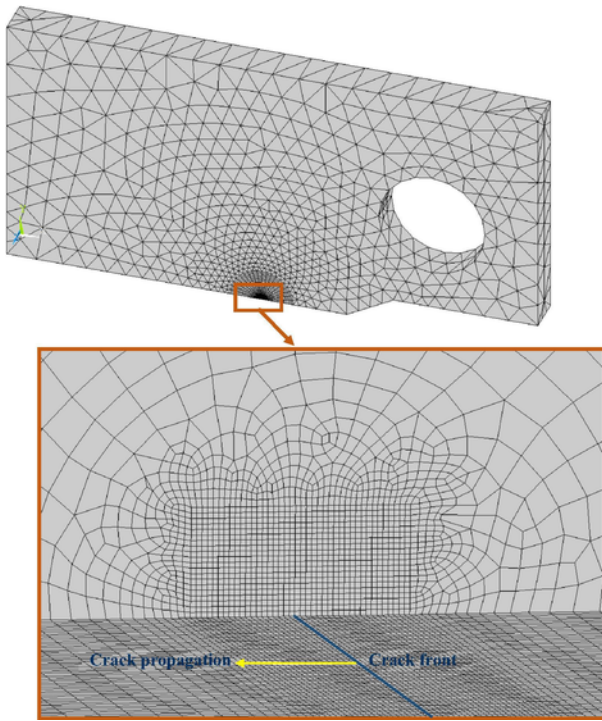


Fig. 2. Finite element model for a CT specimen with straight crack front, $b = 9\text{ mm}$ and $K_{Nl} = 25\text{ MPa m}^{1/2}$.

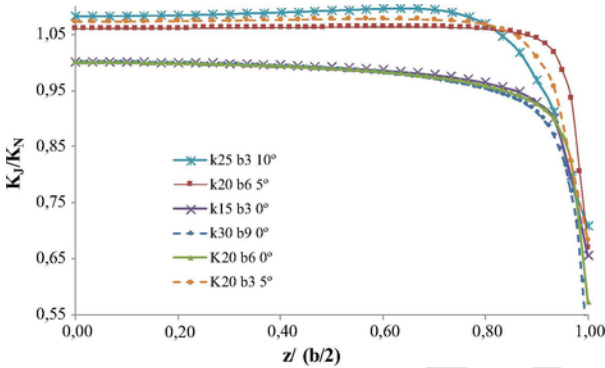


Fig. 3. Differences in stress intensity results in 3D fracture simulations (K25 b3 10° means $K_{Nl} = 25\text{ MPa m}^{1/2}$, $b = 3\text{ mm}$, angle of curvature of the crack front $\alpha = 10^\circ$).

fluence of key factors (mesh density, number of cycles, performance curves, K_{max} , R) on the opening or closure results in both two- and three-dimensional models [16,37]. However, despite good experimental correlations, the results did not consider the heterogeneous distribution of the stress intensity factor across the thickness. One of the author's conclusions was that we can no longer ignore that there is a relationship with K_{max} , which, while it is not estimated to be very large, may be capable of establishing some relationship with the thickness.

To advance in this study two lines of investigation have been developed. On one hand, Camas et al. [38–40] used three-dimensional fatigue models to study the influence of thickness and curvature by analysing plasticised regions and also fitted numerical parameters to determine the crack opening and closure. They upheld the assumption that loading was uniformly distributed across the thickness in order to circumnavigate cross-influences between the two effects. On the other hand, a method of calculation was developed and the K distribution analysed across the entire thickness for numerical fracture simulations. Garcia-Manrique et al. [41–44] have presented some recommendations for calculating K and analysing its influence in function of thickness, the scale of the applied load and the crack front curvature.

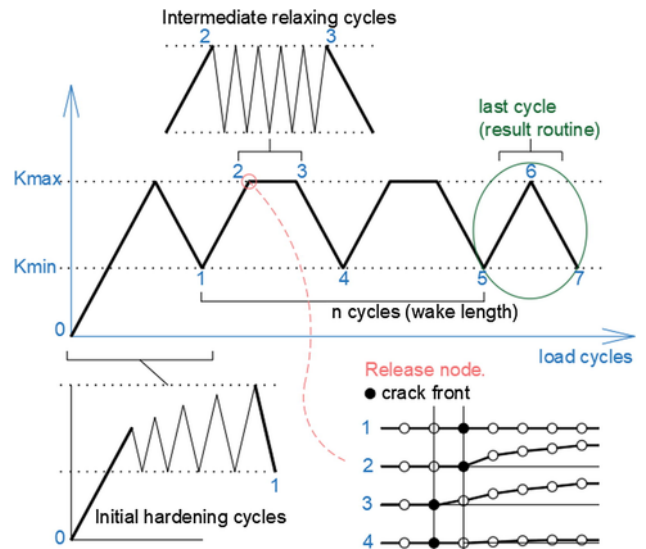


Fig. 4. schematic resume of the methodology used for the simulation of crack growth in fatigue models.

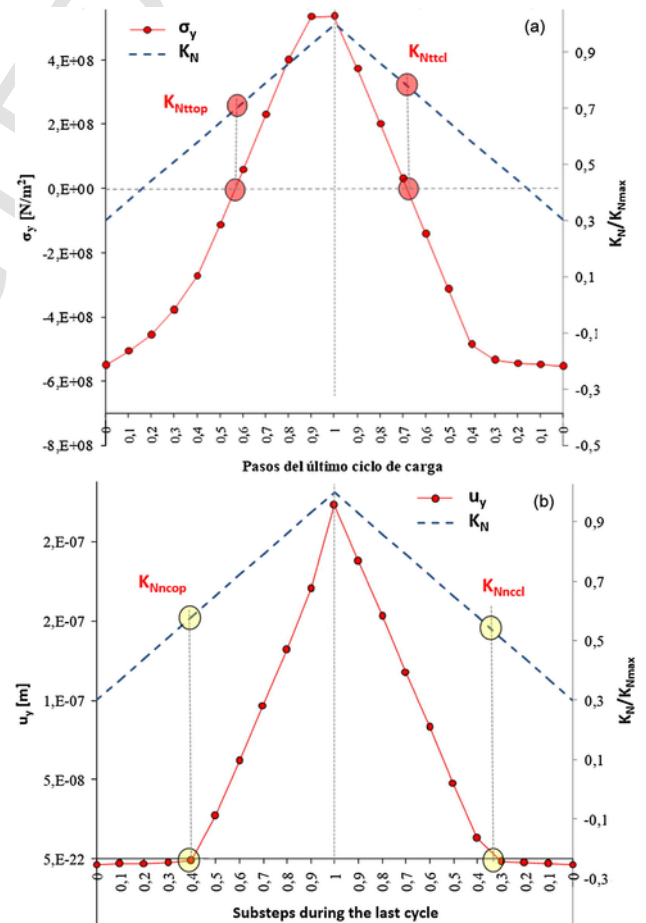


Fig. 5. Procedure for the numerical determination of the moment of opening and closure of the crack and the K_{op} and K_{cl} calculation. (a) Based on stress criteria (K_{Nl}). (b) Based on displacement criteria (K_{Nl}).

This paper presents the first results concerning the cross-over between these two lines of research. We shall analyse the correction applied to the numerical calculation of crack closure by introducing the variable K distribution across the crack front. This heterogeneous dis-

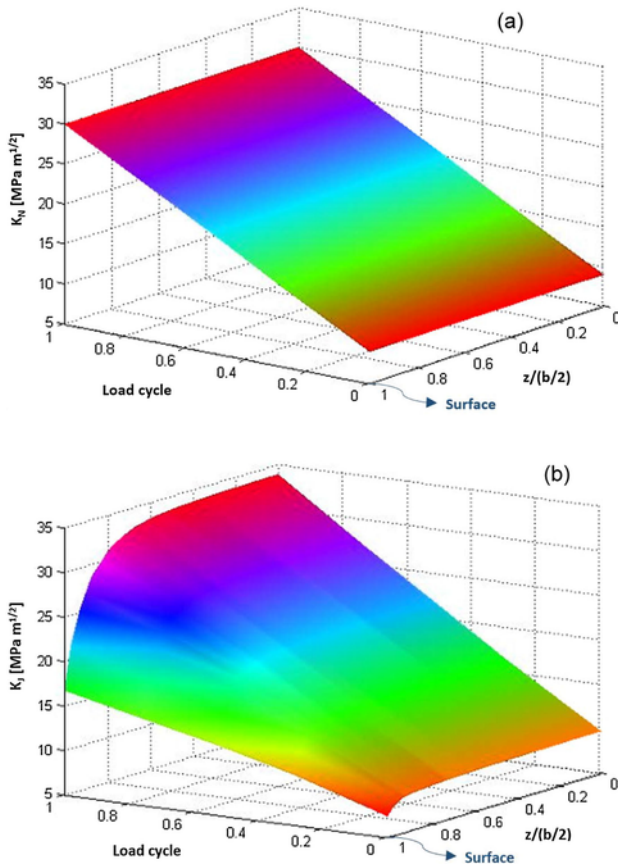


Fig. 6. K value depending on the position of the node in the crack front and the moment of the load cycle. (a) Corresponding to a homogenous distribution (K_N). (b) Corresponding to a results obtained in fracture simulations using J-integral ($K_J(z, K_N)$).

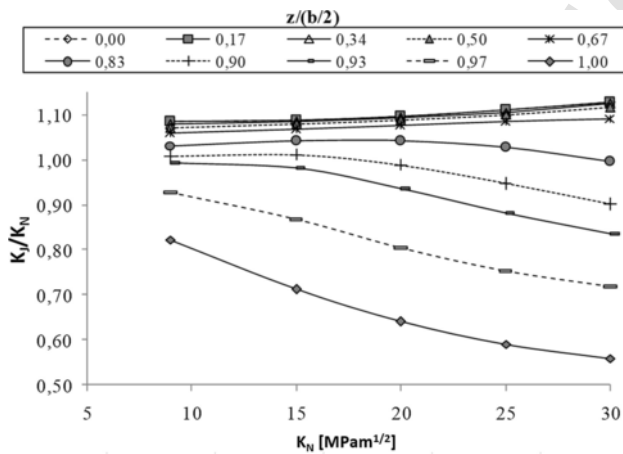


Fig. 7. Evolution of K_J according to K_N for different nodes of the crack front ($b = 3\text{ mm}$ and straight front). The legend identify the node according to the relative position to the midplane.

tribution is also dependent on the degree of loading applied [43] and may therefore have a different influence during each step of the loading or unloading process. We put forward a method for correcting existing data collated from previous fatigue simulations and analyse the significance of these data in terms of detecting crack closure and simulating crack growth rate.

In the second section of the paper we present a compilation of the main aspects of the different numerical simulations, both original and current ones. In next sections we proceed to analyse the parameters susceptible of correction and we present results of this influence in

Table 2

Polynomial trend functions of (K_J/K_N) for some positions of crack front ($b = 3\text{ mm}$, $a = 20\text{ mm}$, straight crack). $x = K_N$.

$z/(b/2)$	$K_J/K_N = f(K_N)$	r^2
0.00	$1.086E-04 x^2 - 2.231E-03x + 1.097$	0.999
0.17	$9.750E-05 x^2 - 1.732E-03x + 1.090$	0.999
0.33	$7.756E-05 x^2 - 8.602E-04x + 1.079$	0.999
0.50	$5.820E-05 x^2 - 1.116E-04x + 1.066$	0.999
0.67	$-2.274E-06 x^3 + 1.276E-04 x^2 - 5.376E-04x + 1.0540$	0.998
0.83	$6.04E-07 x^4 - 5.42E-05 x^3 + 1.47E-03 x^2 - 1.43E-02x + 1.08$	0.999
0.90	$1.179E-05 x^3 - 1.022E-03 x^2 + 2E-02x + 0.902$	1.000
0.93	$2.5E-05 x^3 - 1.7E-03 x^2 + 2.75E-02x + 0.865$	1.000
0.97	$2.06E-05 x^3 - 1.11E-03 x^2 + 7.56E-03x + 0.933$	1.000
1.00	$3.89E-04 x^2 - 2.78E-02x + 1.04$	1.000

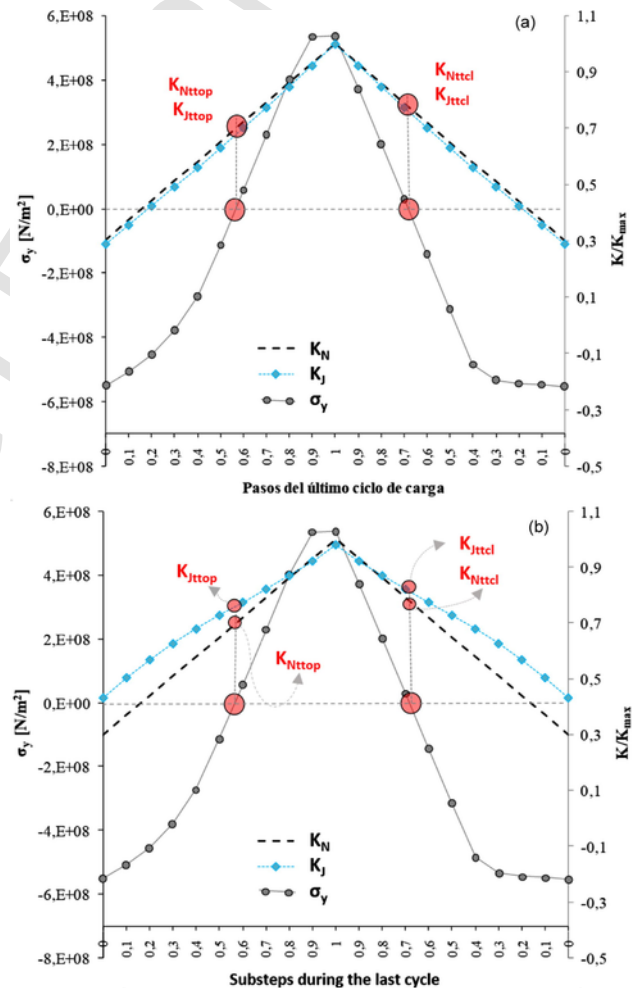


Fig. 8. Correction proposed for the numerical determination of the moment of opening and closure of the crack and the K_{ttop} and K_{tcl} calculation. (a) Node in the midplane. (b) Node in the surface.

PICC determination and in crack growth rate. Finally, we resume some recommendations in the conclusion section.

2. Finite element models review

In this paper, references to results from different numerical models are used. Initial fatigue models were simulated with ABAQUS and recent simulations in fatigue and fracture, with the ANSYS software. In this section we present a review of main numerical aspects that are es-

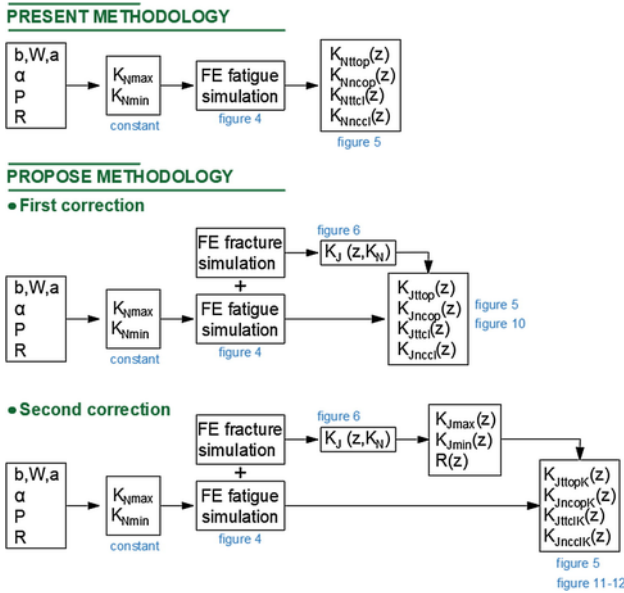


Fig. 9. scheme of the present and proposed simulation methodology.

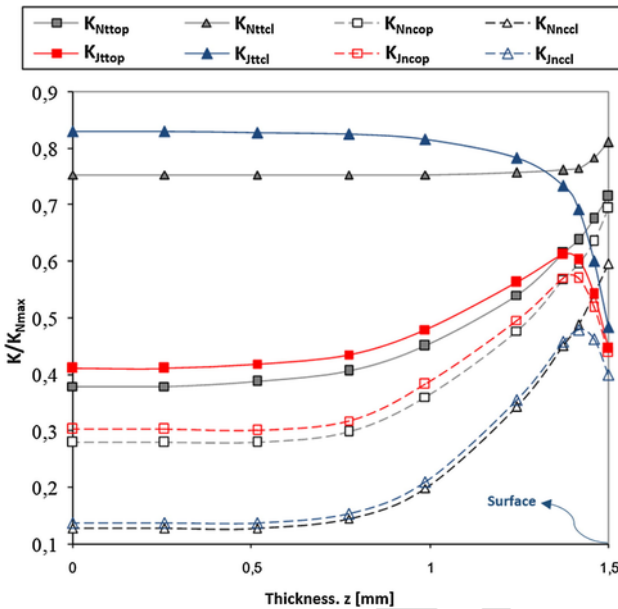


Fig. 10. K_{op} and K_{cl} results along the thickness. Comparison of previous results with the new proposed methodology. All dates are nondimensionalized by the nominal maximum load (K_{Nmax}). Fatigue simulation with $K_{Nmax} = 30 \text{ Mpa m}^{1/2}$, $R = 0.1$, $b = 3 \text{ mm}$.

sential to validate them and to detect the PICC and K values according to the methodologies developed by the authors.

2.1. Geometry and material

All the models correspond with a CT compact tension specimen ($W = 50 \text{ mm}$) appropriate for mode I loading. Long cracks ($a = 20 \text{ mm}$) and thickness ranging from $b = 3$ to 9 mm were modelled. Due to the symmetry of the problem only a quarter of its geometry is necessary, so boundary conditions of symmetry are applied both the middle and the crack plane (Fig. 1).

The material modelled has been Al-2024-T351 aluminium alloy ($E = 75.3 \text{ GPa}$, $\sigma_{yd} = 470 \text{ MPa}$, $K' = 685 \text{ MPa}$, $n' = 0.073$ being K' and n' parameters in the Ramberg-Osgood yielding model) with isotropic hardening rule as plastic behaviour. The results selected have

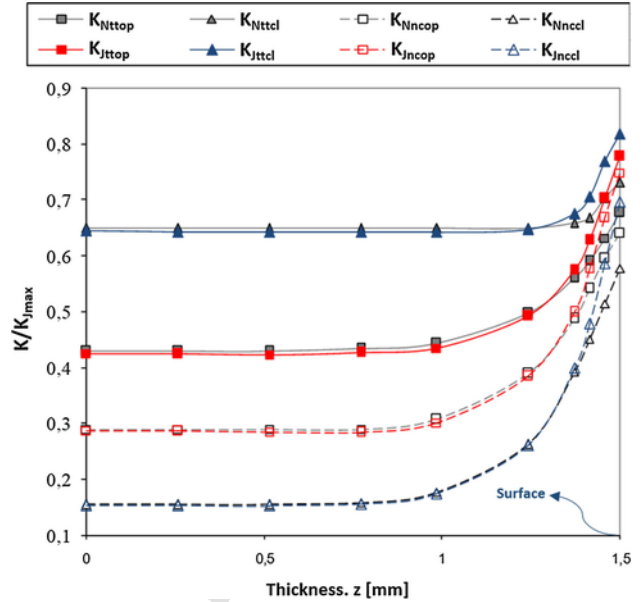


Fig. 11. K_{op} and K_{cl} results along the thickness. Comparison of previous results with the new proposed methodology. All dates are nondimensionalized by the K_{max} distribution through thickness (K_{Jmax}). Fatigue simulation with $K_{Nmax} = 20 \text{ Mpa m}^{1/2}$, $R = 0.1$, $b = 3 \text{ mm}$.

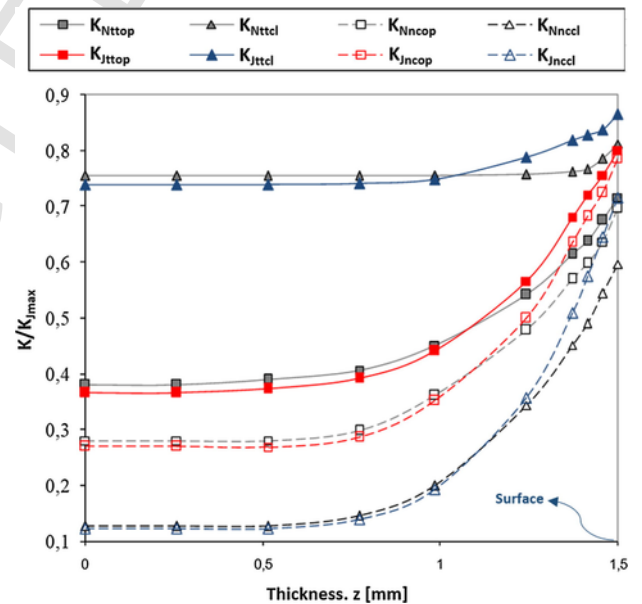


Fig. 12. K_{op} and K_{cl} results along the thickness. Comparison of previous results with the new proposed methodology. All dates are nondimensionalized by the K_{max} distribution through thickness (K_{Jmax}). Fatigue simulation with $K_{Nmax} = 30 \text{ Mpa m}^{1/2}$, $R = 0.1$, $b = 3 \text{ mm}$.

been those with weak hardening ($H/E = 0.003$ where H and E are the slopes of the plastic and elastic line). However, the influence in crack closure results, and the corrections we propose, is similar to ratios below $H/E = 0.03$ with isotropic plastic behaviour [37,42].

2.2. Meshing

The mesh density around the crack front is always one of the main parameters to validate any numerical model. The gradients of the results in this zone have to be properly obtained. In our simulations [16,39,41-45] the element type used is linear cubic one (8 nodes) with full-integration method. The element size both in the crack front (t_{mez})

and crack propagation direction (t_{mex}) has influence in the accuracy of the results, especially in the plasticity crack-closure phenomenon [33,37,46], but also in the stress intensity factor distribution (K) [42]. Both Gonzalez-Herrera and Zapatero (2008) [47] for PICC modelling and Garcia-Manrique et al. (2017) [42] for K, presented recommendation of minimum element size related to the Dugdale's plastic zone size (r_{PD}) and the specimen thickness (b) in order to obtain similar accuracy levels in simulations with different maximum loads and geometries. The element shape ratio is also limited, so exists an additional relation between t_{mez} and t_{mex} .

Fatigue tri-dimensional simulations of PICC [47] were modelled with $t_{mex} < (r_{PD}/90)$, $t_{mez} = 10 \mu m$ and a shape ratio below 6 to 1. This mesh was based on the previous studies of the influence of minimum element size on 2D fatigue crack closure simulations [37] and was limited by the computational cost. Nowadays, the devices present much greater capabilities and a new calculation campaign has been carried out to validate the 2-D study in a 3-D series of simulations. The results obtained indicate that the mesh density were adequate though it would be recommended to reduce it in through thickness direction and to increase in the x-axis one. Fracture tri-dimensional simulations to obtain K [43] were modelled with $t_{mex} < (r_{PD}/30)$, $t_{mez} < (b/80)$ and a shape ratio below 4 times.

The minimum element sizes are defined for the meshing of the vicinity of the crack front (t_{mex}) and the surface (t_{mez}). It is usual to work with a progressive mesh to reduce the number of nodes, were the smaller will be situated in the intersection between the crack and the free surface of the specimen. In Table 1, mesh design parameters from models related to this article are resumed. In Fig. 2 shows the mesh density in the region near the crack front in the case of a fatigue simulation of $K_{Nmax} = 20 \text{ Mpam}^{1/2}$, $b = 6 \text{ mm}$, $R = 0.3$, $a = 20 \text{ mm}$.

The contact between the faces of the crack is also a critical phenomenon in the crack advance simulation. It is an important non-linearity. It is necessary to adjust the penetration value correctly and solve the associated numerical problems of convergence. In all the fatigue models an exponential pressure-clearance relationship were used with a maximum penetration under 10^{-11} m .

2.3. Load distribution along the thickness. K

Throughout the development of the text and the figures of the paper, we present different meanings of the stress intensity factor according to the following nomenclature and the methodology of their numerical calculation. We emphasize the difference between the so-called K_N and K_J . The first one (K_N) refers to the K value predicted for the specimen type through the known relation of Eq. (5).

$$K_N = \frac{P}{b\sqrt{w}} \left\{ \frac{2 + \frac{a}{w}}{\left(1 - \frac{a}{w}\right)^{2/3}} \cdot \left[0.886 + 4.64 \cdot \left(\frac{a}{w}\right) - 13.32 \cdot \left(\frac{a}{w}\right)^2 + 14.72 \cdot \left(\frac{a}{w}\right)^3 - 5.6 \cdot \left(\frac{a}{w}\right)^4 \right] \right\} \quad (5)$$

It is a value contrasted in the study of fatigue life for CT specimens and depends mainly on the geometry and the maximum load level applied (P). We call it nominal. The second one (K_J) includes the three-dimensional evaluation of the load distribution along the thickness, namely is a function of z and can be denoted as $K_J(z)$. It refers to the K calculated by the methodology developed which we can summarize in the next points:

- It is obtained through the J-integral applying domain integrals around the crack front by an ANSYS code subroutine.
- The relation between the J-integral evolution and K_J assume plane strain hypothesis.
- K_J is influenced by the number of element included in the integration, the minimum element size, the direction of crack propagation influence, etc. This methodology has been studied and can be consulted in previous works [41–43].

Throughout recent years, we have accumulated a large number of simulations on $K_J(z)$ in fracture models, analysing the influence of thickness, load and/or curvature. Today, some of the main conclusions are evident although they have not yet been transferred to other cases of study. Among them, it is worth remembering for its applicability in this paper, three qualitative concepts:

- The K_J distribution is not homogeneous, however, the overall are similar to the nominal one. So the method distributes the same amount of load along the crack front [42].
- Both the load level and the thickness have influence in the way that this distribution happens. The shape of the results curve cannot be extrapolated and there is a cross-influence between these parameters [43].
- Recent simulations with several curvatures presents conclusions in the line of an important influence also with this factor. We study the curvature through a parameter that identifies the angle of curvature with respect to the outer face (α).

Fig. 3 presents some of these simulations and highlights the important differences in the distribution of results when we vary the parameters described. We can summarized that, in a broad sense, K_J is a function of many parameters, $K_J = f(z, K_{Nmax}, b, \alpha)$, not only $K_J(z)$.

2.4. Numerical simulation of crack closure (K_{op}/K_{cl})

The correct simulation of the crack growth under fatigue, in such a way that allows us to study its effect in areas very close to the crack front, presents a great difficulty even with the current computing capabilities. We have developed and contrasted models where the main parameters of the process have been analysed [37,47,48]: element size, plastic wake generated, opening and closure criteria, etc. In this section we will focus on the growth methodology of the last cycles and how the opening and closure of the crack is determined.

In all the results presented in this paper, the models have the following fundamental characteristics (a schematic outline is shown in Fig. 4):

- The plastic wake generated has been longer than $0.5 r_{PD}$ to guarantee the convergence in the numerical results of opening and closure.
- Tensile tip (K_{tt}) and node-contact (K_{nc}) criteria have been applied. Though the first one seems to have better accuracy, both of them are widely used.
- The nodes are released at the moment of maximum load of each loading cycle. In this moment the boundary conditions change, the node is free, and the crack consequently advances a size equal to the element size of that region.
- Steps of relaxation and initial hardening are used to improve convergence.
- One loading cycle (load, node release and unload) is modelled between nodes releases. The hardening level of the material is low enough so no more cycles are needed.

Once the crack has reached the desired length, we introduce a last cycle of loading and unloading with no variations in the boundary conditions. During this two steps, a numerical routine retrieves the values

of the control variable established in the chosen opening criterion (displacement in K_{nc} or stress in K_{tt}) for all the nodes belonging to the crack front. Enough equidistant substeps are set to have accurate data.

The routine monitors the evolution of the results on each loading slope and identify the moment in which the variable changes sign. So we get opening (negative to positive) and closure (positive to negative) moments. To translate this to values of K_{op} and K_{cl} , the value of K applied in the specimen is identified for that moment. For this, as shown in the figure, it is correlated with the applied loading step that in our models oscillates between K_{min} and K_{max} .

Fig. 5 presents this procedure for tip tensile (K_{tt}) and node contact (K_{nc}) criterion. In the figure, the x-axis indicates the substeps made during the last two load cycles, where the data of the reference variables are taken. The ordinate axes shows both the value of this variable (left axis) and the value of the K_N during the process (right axis).

3. Influence of inhomogeneous distribution of K along the thickness in K_{OP} and K_{CL}

First at all, we will briefly outline the complexity of the problem we are dealing with (in the next section, a scheme is included in Fig. 9 to help to understand the present and proposed simulation process). Once the thickness of the specimen and the curvature is established, the problem is defined by K_{Nmax} and R (and consequently K_{Nmin}). We can simulate a FE fatigue crack closure problem and obtain the different opening and closure points (K_{Ntop} , K_{Ncop} , K_{Nttcl} and K_{Nncl}) which are dependent of the position along the thickness (z) and will we denote as $K_{Nopcl}(z)$ on the following discussion in order to represent the four criteria. Based on these results we can obtain $\Delta K_{Neff}(z)$ along the thickness.

The described methodology allows to determine with good accuracy the moments of opening and closure in three-dimensional models and the values of crack opening and closure.

However, if we analyze the process, the values of K_{op} and K_{cl} obtained correspond to those of applied load and do not take into account the actual distribution along the crack front. For each node of the crack front, the reference variable is compared with the same linear slope that connects K_{min} and K_{max} . So it is the nominal value (K_N) at that instant and therefore, indirectly, introduces the characteristic that this is constant along the crack front. As we discuss in the introduction this could result in errors when we require to study parameters very dependent on the three-dimensional effects next to the front, such as growth criteria to visualize the evolution of the crack front shape.

To include the effect of real load distribution along the thickness, 3-D effects in K calculation have to be introduced. So we propose to change the reference of K , so that instead of K_N formulation, we can correct $K_{Nopcl}(z)$ in terms of $K_j(z)$, obtaining $K_{jopcl}(z)$. The curves of results not only cease to be homogeneous along the thickness, but vary depending on the moment of the cycle in which we are (load level influence) and the shape of the crack (angle of curvature influence).

However, we must recall that $K_j(z)$ is valid for a certain K_N (for instance K_{Nmax}), and if we want to make this correction properly we must include the K_N dependence observed in K_j and so consider the function $K_j(z, K_N)$.

The Fig. 6 shows an example where this aspect can be clearly observed. It presents the load distribution along the thickness of a loading and unloading cycle. The simulation parameters were $a = 20$ mm, $b = 3$ mm, $R = 0.1$, $K_{Nmax} = 30$ MPam^{1/2} and straight crack front. On the one hand we have the loads applied throughout the cycle between K_{Nmin} and K_{Nmax} . In the horizontal axes, the substeps of the load cycle and the position with respect to the thickness of the specimen are represented. If we project them directly to the crack front we would have a constant and identical slope for all the nodes. On the other hand (K_j) we have a surface generated from a series of fracture simulations for K_N values between $K_{Nmin} = 3$ MPam^{1/2} and $K_{Nmax} = 30$ MPam^{1/2}.

This second surface (K_j) of results incorporates both the influence in K of the position of the node (z) and of the K_N . It is expected that these behavioral differences have an influence on the calculation of the opening and closure according to the previous methodology. This influence is evaluated by the correction of previous fatigue simulation results.

A procedure to incorporate the $K_j(z, K_N)$ is proposed and applied to two cases: The first of these was the aforementioned $b = 3$ mm, $R = 0.1$ and $K_{Nmax} = 30$ MPam^{1/2}. The other was $b = 3$ mm, $R = 0.1$ and $K_{Nmax} = 20$ MPam^{1/2}, where K_N oscillate between 2 and 20 MPam^{1/2}. So, it is necessary to determine the distributions of K_j for that range of load.

In order to achieve this, as shown in Fig. 7, the evolution of K_j according to K_N has been simulated for the same node positions along the thickness considered in the existing fatigue models. These curves have been analyzed and approximated by polynomial trend functions. This functions (Table 2) are incorporated to a subroutine to identify what is the portion of load in each node for each moment of the cycle.

Taking the previous functions as a reference, the routine correlates the moment of opening and closure of the fatigue models with a new value of K corresponding this time to these K_j distributions. To visualize this, the Fig. 8 shows the nominal loading and unloading ramps versus those calculated according to the previous procedure for two thickness positions: midplane and surface plane.

As expected, the influence of the correction in the midplane of the specimen is no significant. The order of the difference is similar to the one we already found between the theoretical value of K (K_N) and the global value obtained by the integral J (K_{tot}) [42]. However, in the surface plane of the specimen there exist appreciable differences in the opening and closure values. The rest of the crack front presents an intermediate behavior between these two extreme nodes.

4. Corrections in K_{OP} and K_{CL} determination

This methodology has been repeated to correct the values of all nodes of the crack front for opening and closure both tensile and displacement method (Fig. 9: first proposed correction).

Fig. 10 summarize the results obtained. Dash lines correspond with node contact criteria and solid lines with tensile criteria. The solution is normalized with respect the K_{Nmax} ($K_{Nmax} = 30$ MPam^{1/2}) as were the results in the original simulations with K_N . Each set of results (K_{top} , K_{cop} , K_{ttcl} and K_{ncl}) are calculated for both the traditional method and the proposed correction, subscripts N and J respectively.

It is observed that the solutions are qualitatively similar until we get closer to the surface where the corrected solutions fall to lower values. In addition, the corrected results are quantitatively superior to the original ones in the interior zones. This effect is more important in the stress analysis criteria.

In our opinion, these variations do not correspond to recognizable phenomena in the PICC. To adapt the methodology, the decision was made to vary the parameter used to nondimensionalize the solution. It is proposed not to use a constant global parameter, but it is more appropriate to introduce the three-dimensional effect of it (Fig. 9: second proposed correction).

In this way each value in each node of the front is nondimensionalized by the value of the distribution along the thickness of $K_{jmax}(z)$ (by a J -integral approach) instead of the constant value of K_{Nmax} . Figs. 11 and 12 presents the same results normalized again.

The results now present greater convergence inside the specimen. In the case of $K_{Nmax} = 20$ MPam^{1/2} are almost identical. In the case of $K_{Nmax} = 30$ MPam^{1/2} the differences are somewhat greater. This implies an influence of the load level on the behavior of the correction. In addition, the behavior of the curves in the region close to the surface is completely modified. In this way the trend is maintained and the results curves are corrected quantitatively, as expected. In spite of this,

important variations continue to be observed in the zone near the surface. All the gradients towards the surface increase considerably.

Another observable consequence is the increase in the convergence of opening and closure values in the surface between the two criteria studied (K_{it} and K_{nc}).

So, the proposed corrections introduce changes in the results, especially quantitative, and especially in the region near the surface, where PICC influence is greater. K_j correction is therefore necessary to adjust the numerical values of opening and closure in a fatigue simulation.

5. Conclusions

In this paper we have analysed the influence of the three-dimensional profile of the stress intensity factor in the numerical determination of crack opening and closure by plasticity. The usual methodology is to identify the moments of opening and closure through a stress intensity factor corresponding to the load level applied at that instant. It is done by the assumption of a K distributed uniformly (K_N). However, when we do not study the total advance of the crack but the evolution of phenomena close to the crack front, this hypothesis subtracts information from the problem. It is well known that K presents a variation along the thickness which depends on factors such as load level or the shape of the front.

To analyse this influence, a methodological correction has been made through the correction of the reference intensity factor used. Instead of K_N we propose the use of the value of $K_j(z, K_N)$ corresponding to each node and to each level of applied load.

For this, results of K_{op} and K_{cl} obtained in previous fatigue simulations are presented and compared with those obtained according to the proposed modification.

The main conclusion is that variations in the corrected results are obtained. The importance of the deviations depends on the position along the thickness. It is more relevant, as expected, in the region close to the surface. The results suggest that there is also an influence on the load ratio R and the value of the maximum load.

This conclusion apply with regard both to the methods of calculations based on control variables of displacement (K_{nc}) and stress (K_{it}). In addition, improved convergence is obtained between the opening ($K_{\text{top}}-K_{\text{ncop}}$) and closure ($K_{\text{itcl}}-K_{\text{nccl}}$).

Acknowledgements

Financial support of Junta de Andalucía through Proyectos de Excelencia grant reference TEP-3244 is also acknowledged

References

- P.C. Paris, F. Erdogan, A critical analysis of crack propagation laws, *Trans. Am. Soc. Mech. Eng. J. Basic Eng.* 85 (1963) 528–534.
- K. Walker, The effect of stress ratio during crack propagation and fatigue for 2024-T3 and 7076-T6 aluminum, in: *Eff. Environ. Complex Load Hist. Fatigue Life*, ASTM STP 462, American Society for Testing and Materials, Philadelphia, 1970, pp. 1–14.
- R.G. Forman, V.E. Kearney, R.M. Engle, Numerical analysis of crack propagation in cyclic-loaded structures, *J. Basic Eng.* 89 (1967) 459–463.
- I.F.C. Smith, R.A. Smith, Fatigue crack growth in a fillet welded joint, *Eng. Fract. Mech.* 18 (1983) 861–869, [https://doi.org/10.1016/0013-7944\(83\)90130-3](https://doi.org/10.1016/0013-7944(83)90130-3).
- W. Elber, Fatigue crack closure under cyclic tension, *Eng. Fract. Mech.* 2 (1970) 37–45.
- W. Elber, The significance of fatigue crack closure, in: *Damage Toler. Aircr. Struct.*, American Society for Testing and Materials, Philadelphia, 1971, pp. 230–242.
- R.O. Ritchie, S. Suresh, C.M. Moss, Near-threshold fatigue crack growth in 2 1/4 Cr-1Mo pressure vessel steel in air and hydrogen, *J. Eng. Mater. Technol.* 102 (1980) 293, <https://doi.org/10.1115/1.3224813>.
- S. Suresh, R.O. Ritchie, On the influence of fatigue underloads on cyclic crack growth at low stress intensities, *Mater. Sci. Eng.* 51 (1981) 61–69, [https://doi.org/10.1016/0025-5416\(81\)90107-5](https://doi.org/10.1016/0025-5416(81)90107-5).
- K.T.V. Rao, W. Yu, R.O. Ritchie, On the behavior of small fatigue cracks in commercial aluminum-lithium alloys, *Eng. Fract. Mech.* 31 (1988) 623–635, [https://doi.org/10.1016/0013-7944\(88\)90105-1](https://doi.org/10.1016/0013-7944(88)90105-1).
- F. Yusof, P. Lopez-Crespo, P.J. Withers, Effect of overload on crack closure in thick and thin specimens via digital image correlation, *Int. J. Fatigue* 56 (2013) 17–24.
- J.D. Dougherty, T.S. Srivatsan, J. Padovan, Fatigue crack propagation and closure behavior of modified 1070 steel: experimental results, *Eng. Fract. Mech.* 56 (1997) 167–187, [https://doi.org/10.1016/S0013-7944\(96\)00103-8](https://doi.org/10.1016/S0013-7944(96)00103-8).
- F. Ellyin, J. Wu, A numerical investigation on the effect of an overload on fatigue crack opening and closure behaviour, *Fatigue Fract. Eng. Mater. Struct.* 22 (1999) 835–847.
- K. Donald, P.C. Paris, An evaluation of ΔS Keff estimation procedures on 6061-T6 and 2024-T3 aluminum alloys, *Int. J. Fatigue* 21 (1999) 47–57, [https://doi.org/10.1016/S0142-1123\(99\)00055-9](https://doi.org/10.1016/S0142-1123(99)00055-9).
- H. Sehitoglu, W. Sun, Modeling of plane strain fatigue crack closure, *J. Eng. Mater. Technol.* 113 (1991) 31, <https://doi.org/10.1115/1.2903380>.
- J. Zapatero, B. Moreno, A. González-Herrera, Fatigue crack closure determination by means of finite element analysis, *Eng. Fract. Mech.* 75 (2008) 41–57, <https://doi.org/10.1016/j.engfractmech.2007.02.020>.
- A. Gonzalez-Herrera, J. Zapatero, Numerical study of the effect of plastic wake on plasticity-induced fatigue crack closure, *Fatigue Fract. Eng. Mater. Struct.* 32 (2009) 249–260, <https://doi.org/10.1111/j.1460-2695.2009.01335.x>.
- K. Vor, C. Gardin, C. Sarrazin-Baudoux, J. Petit, Wake length and loading history effects on crack closure of through-thickness long and short cracks in 304L: Part II – 3D numerical simulation, *Eng. Fract. Mech.* 99 (2013) 306–323, <https://doi.org/10.1016/j.engfractmech.2013.01.014>.
- F.V. Antunes, L. Correia, D. Camas, R. Branco, Effect of compressive loads on plasticity induced crack closure, *Theor. Appl. Fract. Mech.* 80 (2015) 193–204, <https://doi.org/10.1016/j.tafmec.2015.09.001>.
- C. Gardin, S. Courtin, G. Bézein, D. Bertheau, H.B.H. Hamouda, Numerical simulation of fatigue crack propagation in compressive residual stress fields of notched round bars, *Fatigue Fract. Eng. Mater. Struct.* 30 (2007) 231–242, <https://doi.org/10.1111/j.1460-2695.2007.01101.x>.
- K. Sadananda, A.K. Vasudevan, Multiple mechanisms controlling fatigue crack growth, *Fatigue Fract. Eng. Mater. Struct.* 26 (2003) 835–845, <https://doi.org/10.1046/j.1460-2695.2003.00684.x>.
- J. Toribio, V. Khari, Plasticity-induced crack closure: a contribution to the debate, *Eur. J. Mech. - A/Solids* 30 (2011) 105–112, <https://doi.org/10.1016/j.euromechsol.2010.11.002>.
- D. Kujawski, Enhanced model of partial crack closure for correlation of R-ratio effects in aluminum alloys, *Int. J. Fatigue* 23 (2001) 95–102, [https://doi.org/10.1016/S0142-1123\(00\)00085-2](https://doi.org/10.1016/S0142-1123(00)00085-2).
- X. Huang, T. Moan, Improved modeling of the effect of R-ratio on crack growth rate, *Int. J. Fatigue* 29 (2007) 591–602, <https://doi.org/10.1016/j.ijfatigue.2006.07.014>.
- F.V. Antunes, T. Sousa, R. Branco, L. Correia, Effect of crack closure on non-linear crack tip parameters, *Int. J. Fatigue* 71 (2015) 53–63, <https://doi.org/10.1016/j.ijfatigue.2014.10.001>.
- N.E. Ashbaugh, Effects of load history and specimen geometry on fatigue crack closure measurements, *Mech. Fatigue Crack Closure*, ASTM STP 982 (1988) 186–196.
- N.A. Fleck, Compliance methods for measurement of crack length, in: K.J. Marsh, R.A. Smith, R.O. Ritchie (Eds.), *Fatigue Crack Meas. Tech. Appl.*, Engineering Materials Advisory Services Ltd, West Midlands, 1991, pp. 69–93.
- S.K. Ray, A.F. Grandt, Comparison of methods for measuring fatigue crack closure in a thick specimen, in: J. J.C. Newman, W. Elber (Eds.), *Mech. Fatigue Crack Closure*, ASTM STP 982, American Society for Testing and Material, Philadelphia, 1988, pp. 197–213.
- W. Yisheng, J. Schijve, Fatigue crack closure measurement on 2024-T3 sheet specimens, *Fatigue Fract. Eng. Mater. Struct.* 18 (1995) 917–921.
- J. Carroll, C. Efstathiou, J. Lambros, H. Sehitoglu, B. Hauber, S. Spottswood, R. Chona, Investigation of fatigue crack closure using multiscale image correlation experiments, *Eng. Fract. Mech.* 76 (2009) 2384–2398, <https://doi.org/10.1016/j.engfractmech.2009.08.002>.
- M. Mokhtarshirzabad, P. Lopez-Crespo, B. Moreno, A. Lopez-Moreno, M. Zanganeh, Evaluation of crack-tip fields from DIC data: a parametric study, *Int. J. Fatigue* 89 (2016) 11–19, <https://doi.org/10.1016/j.ijfatigue.2016.03.006>.
- L.P. Pook, A 50-year retrospective review of three-dimensional effects at cracks and sharp notches, *Fatigue Fract. Eng. Mater. Struct.* 36 (2013) 699–723, <https://doi.org/10.1111/ffe.12074>.
- S. Roychowdhury, R.H. Dodds, R.H. Dodds Jr., R.H. Dodds, A numerical investigation of 3-D small-scale yielding fatigue crack growth, *Eng. Fract. Mech.* 70 (2003) 2363–2383, [https://doi.org/10.1016/S0013-7944\(03\)00003-1](https://doi.org/10.1016/S0013-7944(03)00003-1).
- C. Gardin, S. Fiordalisi, C. Sarrazin-Baudoux, J. Petit, Numerical simulation of fatigue plasticity-induced crack closure for through cracks with curved fronts, *Eng. Fract. Mech.* 160 (2016) 213–225, <https://doi.org/10.1016/j.engfractmech.2015.11.023>.
- C. Gardin, S. Fiordalisi, C. Sarrazin-Baudoux, M. Gueguen, J. Petit, Numerical prediction of crack front shape during fatigue propagation considering plasticity-induced crack closure, *Int. J. Fatigue* 88 (2016) 68–77, <https://doi.org/10.1016/j.ijfatigue.2016.03.018>.
- W. Sun, H. Sehitoglu, Residual stress fields during fatigue crack growth, *Fatigue Fract. Eng. Mater. Struct.* 15 (1992) 115–128.
- A. Gonzalez-Herrera, Determinación numérica de las tensiones de apertura y cierre de grieta en fatiga, *Phd Thesis Universidad de Málaga*, 2004.
- A. González-Herrera, J. Zapatero, Influence of minimum element size to determine crack closure stress by the finite element method, *Eng. Fract. Mech.* 72 (2005) 337–355, <https://doi.org/10.1016/j.engfractmech.2004.04.002>.
- D. Camas, J. Garcia-Manrique, B. Moreno, A. Gonzalez-Herrera, Numerical modeling of three-dimensional fatigue crack closure: mesh refinement, *Int. J. Fatigue* (2018) <https://doi.org/10.1016/j.ijfatigue.2018.03.035>.

- [39] D. Camas, J. Garcia-Manrique, A. Gonzalez-Herrera, Crack front curvature: Influence and effects on the crack tip fields in bi-dimensional specimens, *Int. J. Fatigue*. 44 (2012) 41–50, <https://doi.org/10.1016/j.ijfatigue.2012.05.012>.
- [40] P. Lopez-Crespo, D. Camas-Pena, A. Gonzalez-Herrera, J.R. Yates, E.A. Patterson, J. Zapatero, Numerical and experimental analysis of crack closure, *Key Eng. Mater.* 385–387 (2008) 369–372.
- [41] J. Garcia-Manrique, D. Camas, P. Lopez-Crespo, A. Gonzalez-Herrera, Stress intensity factor analysis of through thickness effects, *Int. J. Fatigue* 46 (2013) 58–66, <https://doi.org/10.1016/j.ijfatigue.2011.12.012>.
- [42] J. Garcia-Manrique, D. Camas, A. Gonzalez-Herrera, Study of the stress intensity factor analysis through thickness: methodological aspects, *Fatigue Fract. Eng. Mater. Struct.* 40 (2017) 1295–1308, <https://doi.org/10.1111/ffe.12574>.
- [43] J. Garcia-Manrique, D. Camas-Peña, J. Lopez-Martinez, A. Gonzalez-Herrera, Analysis of the stress intensity factor along the thickness: the concept of pivot node on straight crack fronts, *Fatigue Fract. Eng. Mater. Struct.* (2017) <https://doi.org/10.1111/ffe.12734>.
- [44] D. Camas, J. Garcia-Manrique, A. Gonzalez-Herrera, Three-dimensional effects in the fracture mechanics of bi-dimensional specimens, 2012.
- [45] D. Camas, J. Garcia-Manrique, A. Gonzalez-Herrera, Numerical study of the thickness transition in bi-dimensional specimen cracks, *Int. J. Fatigue* 33 (2011) 921–928, <https://doi.org/10.1016/j.ijfatigue.2011.02.006>.
- [46] K. Solanki, S.R.R. Daniewicz, J.C.C. Newman, A new methodology for computing crack opening values from finite element analyses, *Eng. Fract. Mech.* 71 (2004) 1165–1175, [https://doi.org/10.1016/S0013-7944\(03\)00113-9](https://doi.org/10.1016/S0013-7944(03)00113-9).
- [47] A. Gonzalez-Herrera, J. Zapatero, Tri-dimensional numerical modelling of plasticity induced fatigue crack closure, *Eng. Fract. Mech.* 75 (2008) 4513–4528, <https://doi.org/10.1016/j.engfracmech.2008.04.024>.
- [48] J. Zapatero, A. Gonzalez-Herrera, Advances in the numerical modelling of fatigue crack closure using finite elements, in: A.F. Lignelli (Ed.), *Fatigue Crack Growth Mech. Behav. Predict.*, Nova Science Publishers, New York, 2009, pp. 83–124.